FINAL PROJECT REPORT

FOR

HIGH-SPEED COUNTING OF PHOTOMULTIPLIER PULSES

(31 JULY 1964 — 30 SEPTEMBER 1964)

Contract No.: NAS 5-9057

Prepared by

APPLIED RESEARCH
DEFENSE ELECTRONIC PRODUCTS
RADIO CORPORATION OF AMERICA
CAMDEN, NEW JERSEY

for

GODDARD SPACE FLIGHT CENTER
NATIONAL AERONAUTICS AND SPACE ADMINISTRATION
GREENBELT, MARYLAND

FINAL PROJECT REPORT

for

HIGH-SPEED COUNTING OF PHOTOMULTIPLIER PULSES

(31 JULY 1964 — 30 SEPTEMBER 1964)

Contract No.: NAS 5-9057

Prepared by

APPLIED RESEARCH
DEFENSE ELECTRONIC PRODUCTS
RADIO CORPORATION OF AMERICA
CAMDEN, NEW JERSEY

for

GODDARD SPACE FLIGHT CENTER
NATIONAL AERONAUTICS AND SPACE ADMINISTRATION
GREENBELT, MARYLAND

SUMMARY

The object of this investigation was to determine the feasibility of detecting and counting random pulses from a photomultiplier at high average rates (to 50 Mc). During the program, a detector and a five-stage counter, using combinational tunnel-diode/transistor circuits, were constructed and evaluated. The results of the tests indicate a pulse-pair resolution of better than 4 nanoseconds with wide dynamic range (20 db). During the evaluation, both well defined multiple pulse outputs and random outputs from a photomultiplier were utilized. Average rates of random events above 30 Mc were successfully measured in tests which simulated conditions to be encountered in the earth-orbit series of experiments planned for the IMP satellite. A program is recommended for the design of prototype units for environmental evaluation, followed by construction of flight test units.

TABLE OF CONTENTS

LIST OF ILLUSTRATIONS

SECTION I

INTRODUCTION

This study was undertaken to determine the feasibility of counting very high rate output pulses from a photomultiplier-detector system. This system will be used in an experiment to be flown in the IMP satellite, F and G earth-orbit series. Basically, the experiment consists of measuring the energy distribution of protons and other ions or "solar wind" in interplanetary space. A highly elliptical orbit is to be flown, so a considerable variation in ion density is expected. Satellite rotation about its axis will provide a means for determining the vector distribution of the ion stream.

Close to the earth, the effects of the magnetosphere are expected to be significant, resulting in considerable variation in the number of detected particles. To optimize the detected signal with respect to relatively fixed background noise sources, it is important that the largest possible ion stream cross-sectional area be monitored by the experiment. One of the factors which is important in determining signal-to-noise ratio is the maximum expected ion density to be encountered. Practical counting limits then determine the size of the aperture to be employed which limits the ion stream cross-sectional area.

Due to the wide range of ion densities expected, it was felt desirable to determine the feasibility of counting events at average rates as high as 50 Mc. The events to be counted were assumed to have the normal Poisson distribution. One of the goals of the study was to determine the feasibility of counting this distribution of events with an 80 to 90 per cent efficiency. To accomplish this requires pulse detection and counting circuitry capable of operating at a rate in excess of 250 Mc.

Briefly, the equipment to be used in the experiment consists of an aperture in the side of the spacecraft followed by a programmable velocity selector and an energy per unit charge selector. The selected particles are accelerated toward a secondary emission device which emits electrons at a 15-kv potential for each primary event. The secondaries are detected by a plastic scintillator coupled to the photomultiplier. The outputs from the photomultiplier are detected by the fast circuitry and counted in a high-speed counter. For additional information concerning this experiment, refer to NASA technical note NASA TN D-2111.[1]

SECTION II

TECHNICAL RESULTS

A. GENERAL

The study was divided into several phases. Initially, work was aimed at developing and breadboarding circuits capable of counting pulses at rates above 250 Mc. In parallel with this effort, a study was made and experiments performed to determine the typical types of pulses to be obtained from representative photomultipliers. The selection of photomultipliers was made from those capable of providing the gain and signal rise time required for the high detection rates. Pulse amplitude variations, pulse pile-up and pulse pair resolution problems were considered in the selection of an adequate pulse shaping and detection circuit to follow the photomultiplier. Next, experiments were performed to test the capability of the circuits at the highest signal rates. These were followed by tests of the circuits with several random pulse sources. Finally, tests were performed at NASA Goddard with laboratory ion sources simulating the expected pulse rates. The laboratory ion sources also will be used to check out the final experiment. Results of the study are presented in the following sections.

B. PULSE STATISTICS

The nature of the events to be counted are expected to follow the normal Poisson statistical distribution. The probability that exactly k events will occur during an interval of time T is given by the Poisson frequency function

$$P_k = \frac{(aT)^k}{k!} e^{-aT} \qquad (1)$$

where a is the average rate of occurrence of events. In a process characterized by this expression, the probability that the interval between successive events

lies between T and T + dT is given by

$$\frac{d}{dT}(1 - e^{-aT}) = ae^{-aT} \tag{2}$$

and the cumulative distribution function is

$$1 - e^{-aT}$$

A plot of this function normalized with respect to the average event frequency, a, is given in Figure 1. The exponential nature of this expression is an indication of the maximum counting rate required to successfully count a specified percentage of the occurring events. With a maximum counting capability of five times the average rate, approximately 82 per cent of the events can be counted. With a counting capability ten times average, approximately 90 per cent of the events can be counted. For a maximum average event rate of 50 Mc, these capabilities correspond to counter rates of 250 and 500 Mc, respectively.

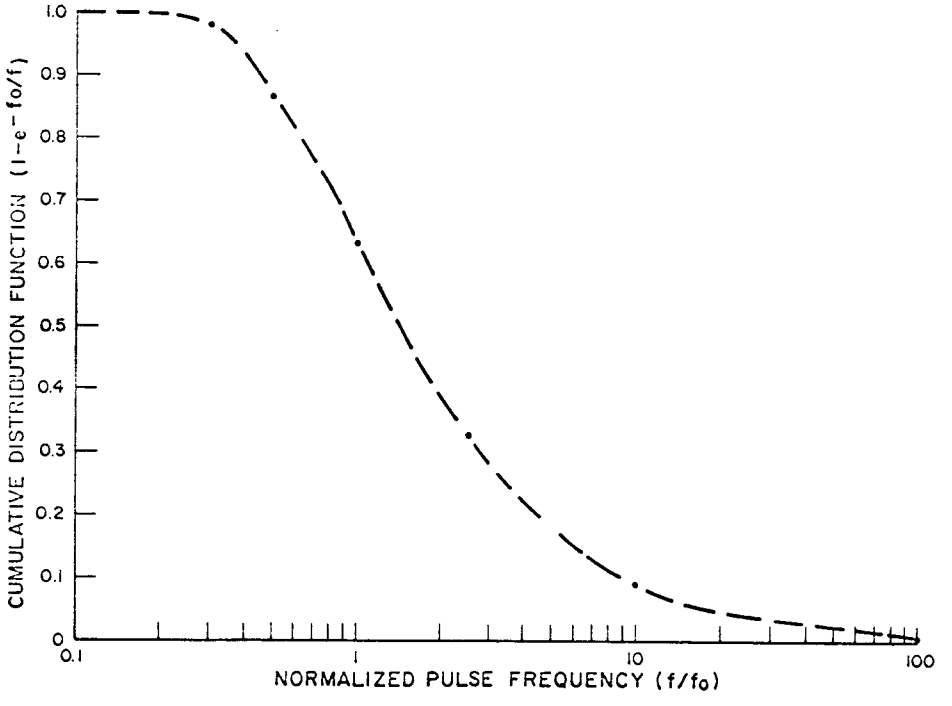

Figure 1. Poisson Distribution Curve

C. PULSE RESOLUTION

Typical output pulse characteristics of photomultipliers are determined by a combination of the input signal and the properties of the specific photomultiplier employed. Tube properties important in high-resolution counting are rise time, photocathode and dynode geometry, and anode geometry. Several photomultipliers are available with output rise times of the order of 2 nanoseconds for well controlled input signals. A typical pulse that can be expected from a tube of this type will have a rise time of approximately 2 nanoseconds with an exponential decay determined mainly by anode and load characteristics. With low value load resistances, the decay time constant, J, will be of the order of 4 nanoseconds. Two pulses arriving close together, therefore, can combine to produce an effect known as pulse pile-up in which the amplitude of the output signal is a function of a previous input as well as the present one. This condition can cause such problems as false pulse detection and failure to detect small amplitude pulses following large ones. Variations in signal amplitude are caused by many factors, such as scattering and energy losses in the scintillator and photocathode.

A worst case for resolving two adjacent pulses occurs when a maximum amplitude pulse is followed by a minimum amplitude pulse. If the system is to respond to both pulses, the threshold must be set so that the minimum amplitude pulse can trigger the detector. This condition requires the exponential portion of the maximum amplitude pulse to decay to some value below the threshold before arrival of the minimum amplitude pulse. For reliable operation the maximum amplitude pulse must decay to a value which is no larger than 0.25 of the minimum amplitude pulse. If the maximum amplitude pulse is denoted by E_{max} and the minimum amplitude by E_{min}, then

$$E_{max}\, e^{-t/J} = 0.25\, E_{min} \qquad (3)$$

Consequently, the minimum pulse separation which the system can resolve under these conditions is obtained from Eq. (3) as

$$t = J \ln 4 \frac{E_{max}}{E_{min}} \tag{4}$$

For an amplitude range of $E_{max}/E_{min} = 10$, the permissible pulse separation is 14.8 nanoseconds, corresponding to a maximum counting rate of 67.5 Mc. The maximum counting rate decreases further as the amplitude range is increased.

The problem of pulse pile-up is remedied by the pulse extraction network. With this network, the pulse decay time equals the pulse rise time. Consequently, for a pulse rise time of 2 nanoseconds, the maximum permissible pulse separation is 4 nanoseconds, corresponding to a counting rate of 250 Mc. By sacrificing 30 per cent of the pulse amplitude, the pulse extraction network can be operated to permit a 3.3-nanosecond pulse separation which corresponds to a counting rate of 300 Mc.

D. PULSED LIGHT SOURCES

To determine the response of a photomultiplier to a narrow pulse of light, two sources were investigated. The first pulsed light source investigated was a gallium arsenide incoherent light-emitting diode. By driving the diode with a high-current pulse of about 100 milliamperes and 1 nanosecond duration, a pulse of light will be emitted in the infrared region.

A 7102 photomultiplier, which was already housed and provided with a bias network, was obtained. This tube has an S-1 spectral response, which is in the infrared region. The main concern was to monitor actual photomultiplier pulses to determine their rise and fall times and to investigate means of providing a random rate pulse source. The diode was located close to the photocathode of the

7102 tube with a small aperture placed in between to limit the usable area on the photocathode. By limiting the photocathode area to a fraction of an inch, better pulse rise times are possible.

The response obtained from the photomultiplier is shown in Figure 2. The rise time of the signal is a function of the input signal to the light-emitting diode, the diode turn-on time and photomultiplier response. The 10 to 90 per cent rise time was approximately 3 nanoseconds with the initial fall time, as shown in Figure 2a, over 10 nanoseconds. The long decay time was found to be due to the recovery time of the gallium arsenide diode. By placing a 5-ohm resistor across the terminals of the diode, the recovery time was reduced considerably. In Figure 2b, the effect of this resistor in rapidly discharging the stored charge of the diode is shown. A diagram of the test set-up used to perform this experiment is shown in Figure 3. In this test, a 50-ohm resistive load was placed across the anode of the photomultiplier. This resistance was found to be effective in discharging the anode capacity of the tube so that the output pulse fall time was not increased. Basically, this experiment served as laboratory verification of the ability to obtain narrow pulse outputs from a photomultiplier with rise times and fall times adequate for counting above 250 Mc.

The second source investigated and constructed was a device for producing narrow pulses in the visible region, suitable for detection with an S-11 photocathode material (spectral response in the violet region). This technique consisted of detecting the spark produced by a mercury-wetted relay contact encased in a glass envelope. This approach, as described by the Berkley Radiation Laboratories[2], can produce a spark of 1 to 2 nanosecond duration and, depending upon the distance between the switch and the photocathode, can cause 1 to 10 electrons to be emitted. A diagram of this source is shown in Figure 4. Difficulties in obtaining a suitable coil to energize the relay and problems in coupling the output to a suitable photomultiplier limited the useful results obtained with this device, although narrow pulses of light were generated and observed using a 7746 photomultiplier.

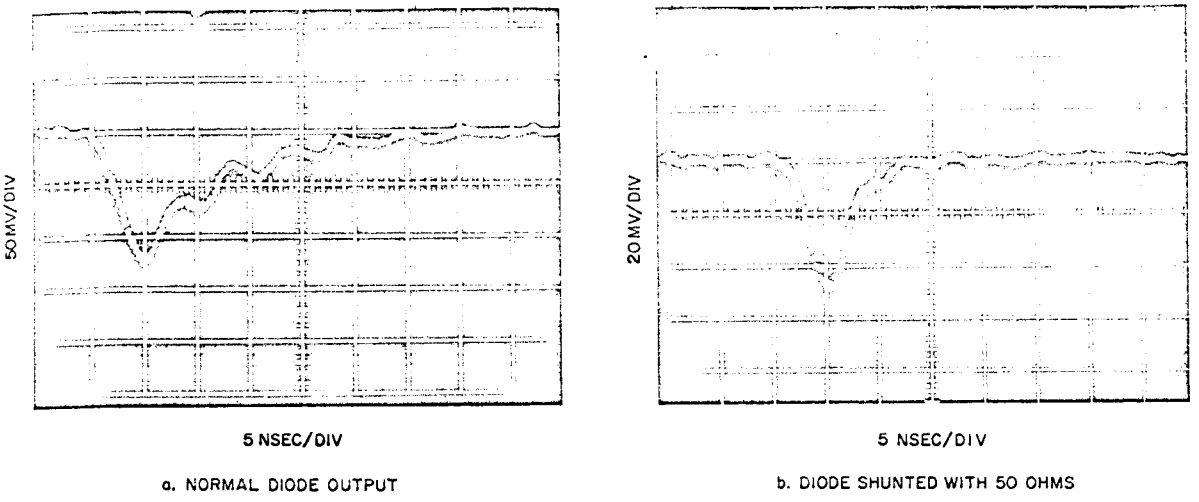

Figure 2. Signal Output from an RCA 7102 Photomultiplier with a GaAs Light-Emitting Diode Source

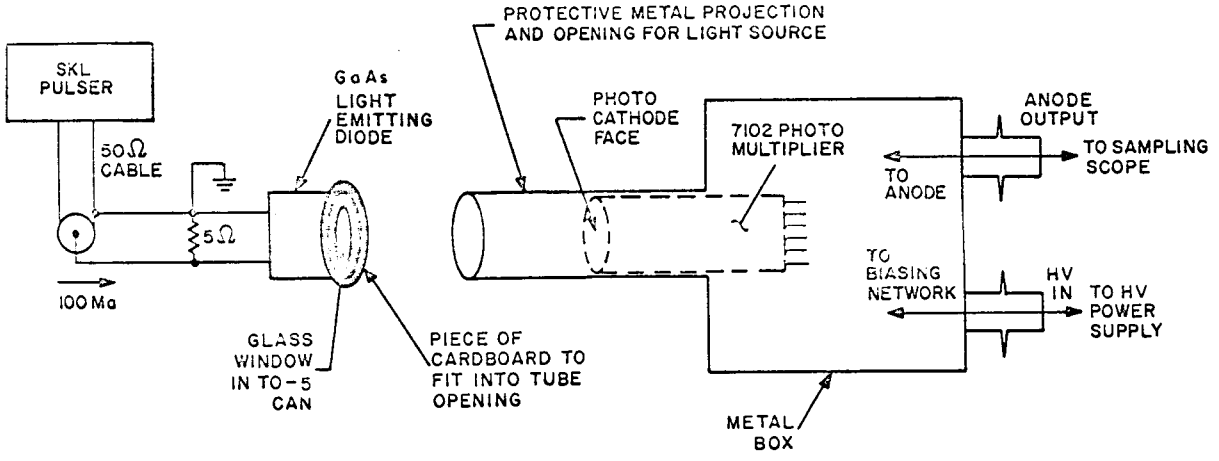

Figure 3. Test Set-Up for Measuring RCA 7102 Photomultiplier Response to GaAs Light-Emitting Diode Source

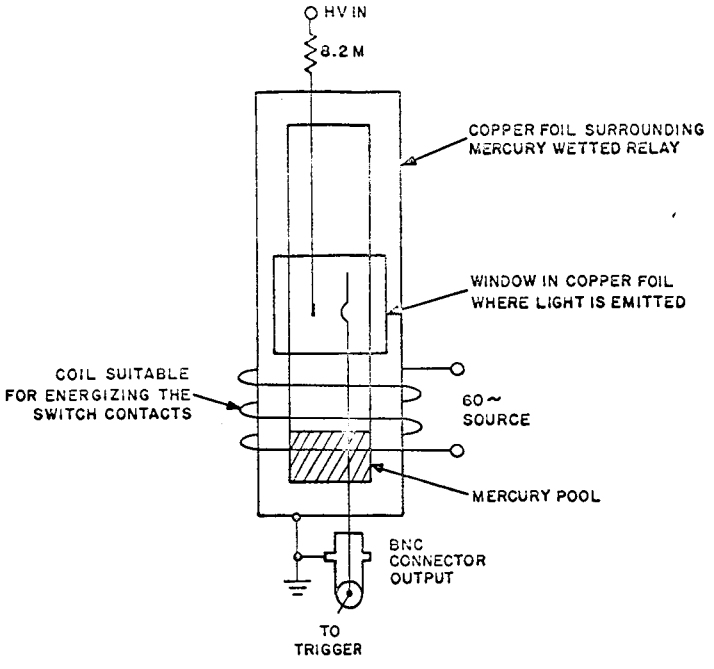

Figure 4. Diagram of Mercury-Wetted Switch Light Source

E. RANDOM PULSE SOURCES

An important aspect of the study was verification of the random pulse counting capability of the detector and counter circuits. To provide as realistic a test as possible, it was desirable to provide a random source at the input to the photomultiplier so that its output would be representative of the actual pulses to be encountered during operation. Several solutions to the problem of random pulse generation were considered, and two selected for additional study and implementation.

The first approach consisted of increasing the single electron dark current emission from the photomultiplier photocathode by stimulation with a low-level diffuse steady light source. To accomplish this, the test arrangement shown in Figure 5 was employed. The set-up consists of a photomultiplier in a light-tight

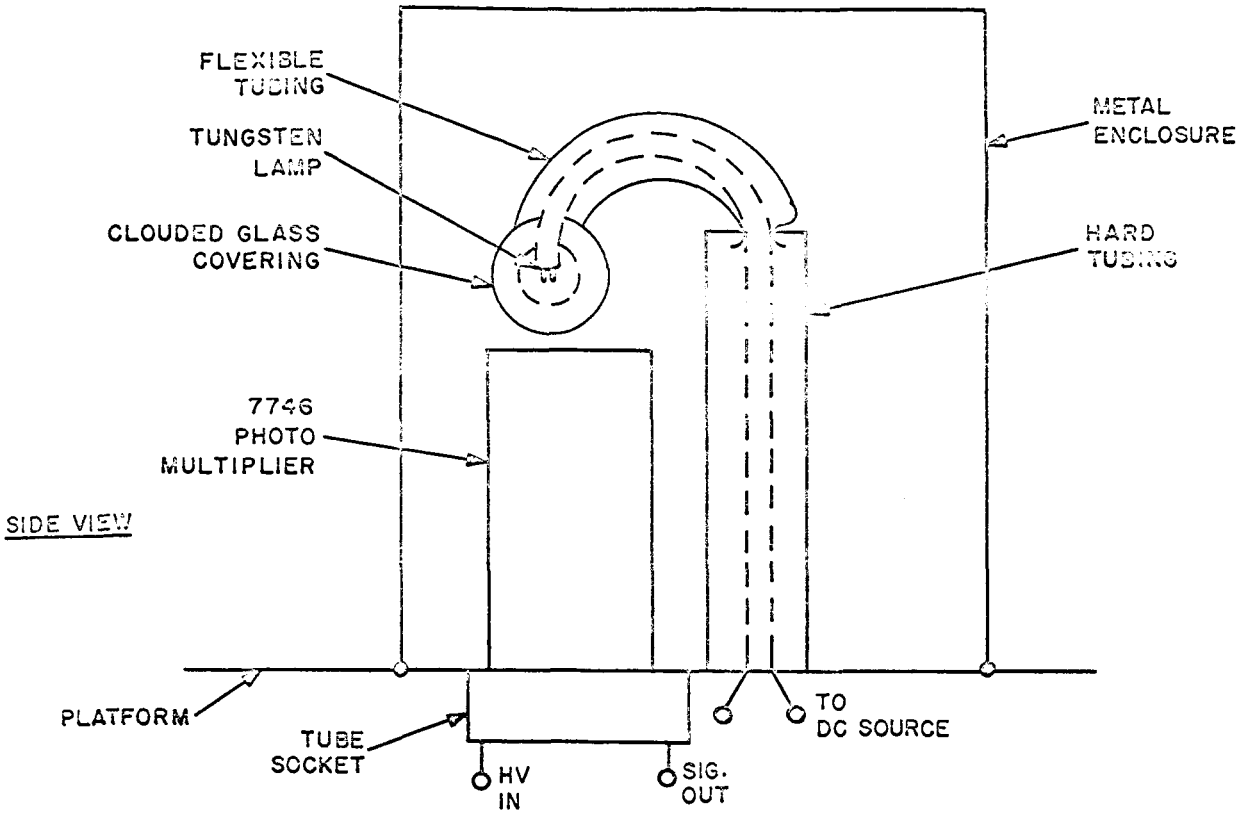

Figure 5. Diagram of 7746 Multiplier Housing and Random Light Source

enclosure with provisions for a tungsten bulb contained in an opaque glass structure. A low-level direct current was passed through the bulb producing photons in the red region. A red source was chosen because of the greater likelihood of producing single electron emission at the photocathode. By varying the current through the bulb, the average number of photons striking the photocathode per unit time could be adjusted, thereby providing a means for adjusting the average rate of the random source. This proved to be a simple, reliable source of random pulses and was used extensively in evaluating the circuits.

A second approach involved the use of a particle source such as a Ni 63 beta source in conjunction with a scintillator and photomultiplier. Tests using this source were made at NASA Goddard and are discussed in a later section of this report.

The problem also existed of observing the random pulses. A method to observe typical random pulses from a photomultiplier tube, either a dark current pulse or a pulse produced by a photoelectron, was devised using a sampling scope. The sampling scope is set on internal trigger. The triggering control on the scope adjusts the threshold bias on a tunnel diode contained in the oscilloscope. By adjusting this threshold, only pulses which exceed this threshold will trigger the sweep of the scope. Each triggered sweep produces a single sample of the pulse that caused the sweep due to the inherent nature of the sampling process. This sample is displayed as a "dot" on the oscilloscope cathode ray tube. Subsequent sweeps have an accumulative delay period before the pulse is sampled and displayed on the tube. In this manner, a complete display is obtained across the face of the tube. When this process is used on pulses with random pulse spacing and amplitude, a composite pulse shape is produced which is the sum of many different sampled pulses. Amplitude variations in the pulse train are shown by considerable spreading of the pulse outline, while repetitive portions are more well defined. (Figure 16 shows a pulse displayed in this manner.)

F. DETECTOR AND COUNTER CIRCUITS

The five-stage counter and the detector circuits were built and tested separately. A schematic of both units is shown in Figure 6. A photograph of the breadboard counter and detector is shown in Figure 7. Both are described in the following paragraphs.

1. Detector

The detector circuit consists of a grounded base NPN silicon transistor with a tunnel diode in its collector. The bias on the transistor and the bias on the tunnel diode control the operating point of the tunnel diode. The transistor is operating in a class A mode and when the negative input pulse arrives, it drives the transistor harder into conduction. This increase in current switches the monostable

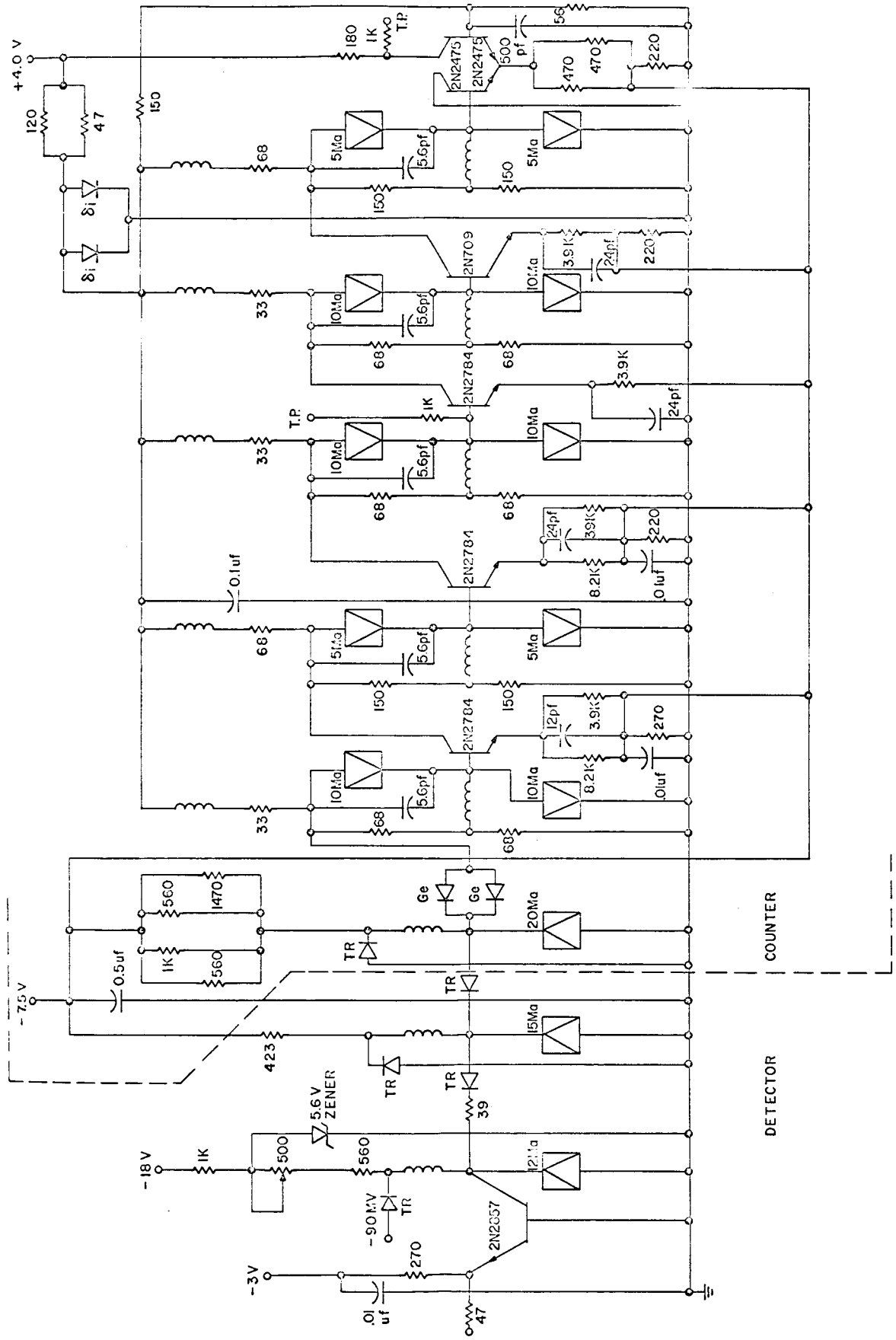

Figure 6. Schematic Diagram of Particle Detector and Counter

Figure 7. Breadboard Detector and Counter

tunnel diode which puts out a narrow pulse. The detector stage is coupled through a resistor and tunnel rectifier to another monostable tunnel-diode stage which fires every time the detector stage receives a pulse. The second monostable tunnel-diode stage was inserted for convenience during the laboratory experiments and is not necessary.

The detector stage was finalized with respect to sensitivity and bias stability. It is very important that, once the threshold setting is fixed, it does not drift any appreciable amount. Any hysteresis effects had to be avoided as well. With respect to sensitivity, the bias on the tunnel diode was brought as close to its threshold as possible and the minimum input pulse needed to fire the tunnel diode was recorded. Ths input pulse was then increased 20 db to assure that no instability resulted. This type of test was also made with a pulse pair separated by 4 nanoseconds.

A minimum amplitude input pulse pair of 30 millivolts peak and 4 nanosecond separation is shown in the upper photograph of Figure 8. The proper operation of the first stage of the counter is shown directly below. The middle photograph illustrates proper operation with input signals of 300-millivolt amplitude. The lower photograph indicates proper operation of the detector with two different pulses; the first, a 350-millivolt pulse and the second, a 30-millivolt pulse delayed by 4 nanoseconds. The last case illustrates a critical condition where a wide dynamic range of over 20 db of input signal is accepted by the detector with 4-nanosecond pulse pair resolution. A slightly longer delay in the response of the first counter stage to the second smaller pulse is noted in this case, although satisfactory operation is still maintained. A calibration curve of the threshold was also recorded and is shown in Figure 9. For each setting of threshold bias, the minimum signal required to activate the detector was recorded. The first stage of the counter was observed again to indicate proper operation.

2. Counter

The counter was designed to work over a wide bias voltage range at speeds as high as 300 Mc. Speed of operation was checked by pulses at a continuous input rate and by pulse-pair inputs. The counter stages are Chow-type flip-flops in the locked-pair configuration. The input to the first counter stage is buffered by the monostable tunnel-diode amplifier circuit after the detector. The output pulse of the monostable amplifier is coupled through a tunnel rectifier into the five-stage counter chain. The input of the counter has another monostable amplifier stage which produces a narrow pulse when triggered. This pulse is coupled into the first stage of the counter and changes the state of the output.

Bias is set so that one tunnel diode is locked in the high state and the other is in the low state. The negative going input pulse momentarily sets both tunnel diodes to the low state. When the tunnel diodes are in their locked condition, current is always flowing in the inductor through the tunnel diode that is in

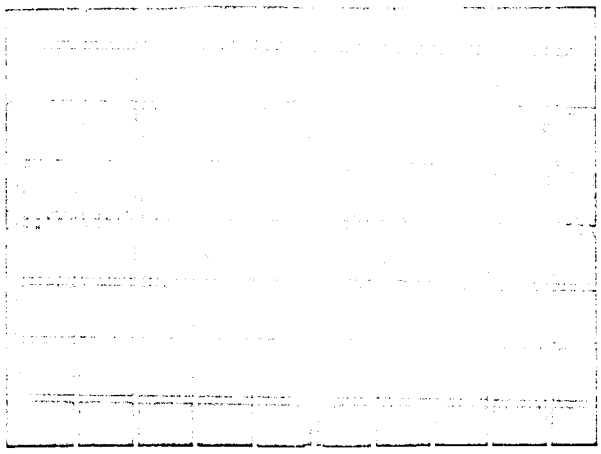

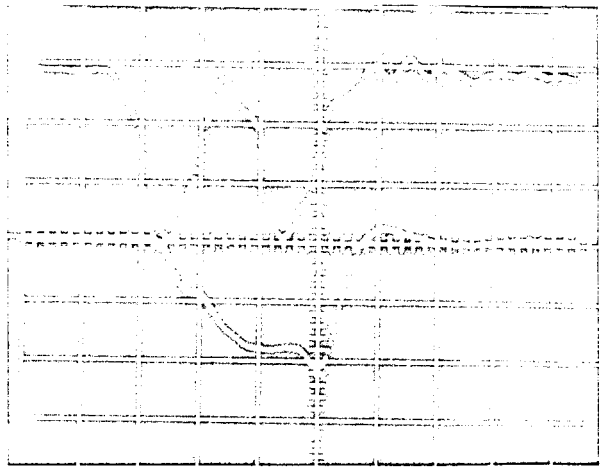

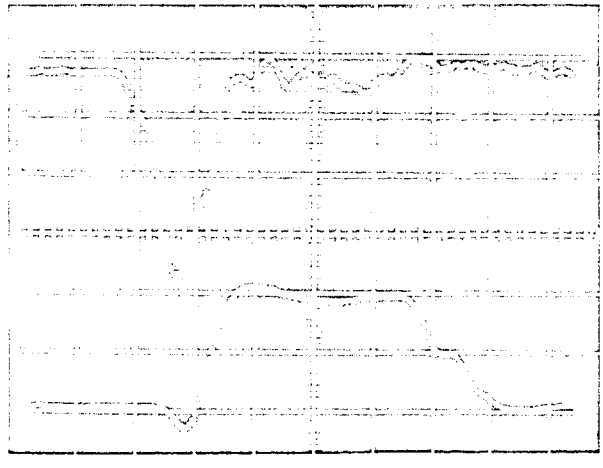

Figure 8. Waveforms of the Sensitivity Tests on the Detector Circuit

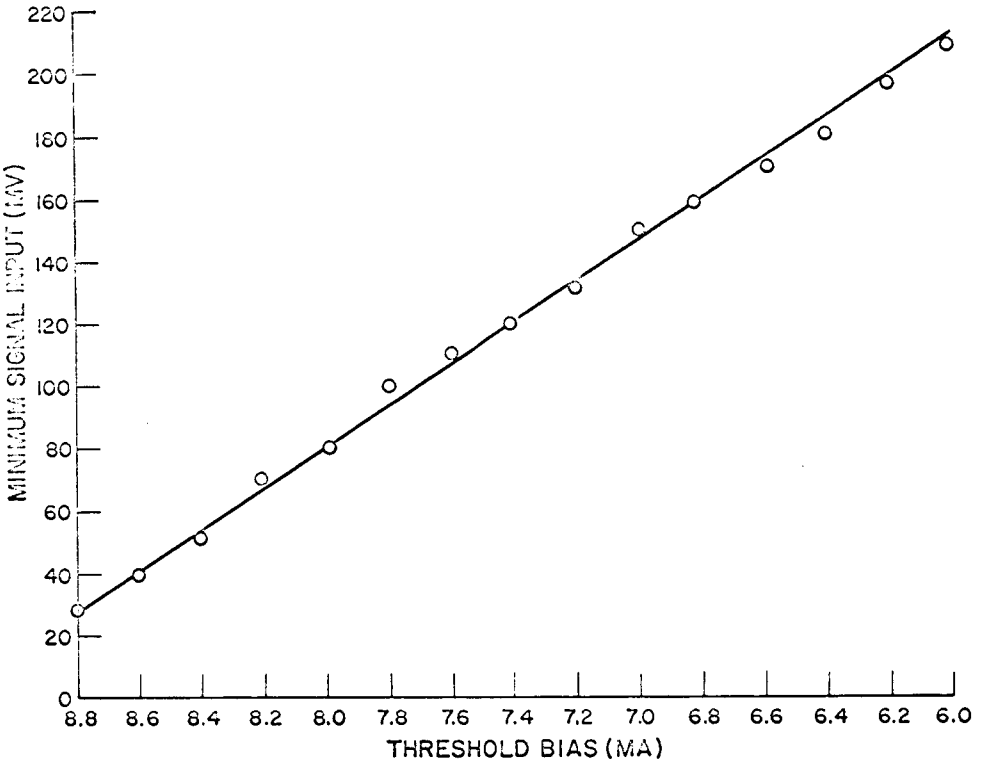

Figure 9. Threshold Calibration Curve

the low state. When the input pulse arrives to momentarily shut off the current from the power supply, this current is maintained through the inductor and the tunnel diode in the low state due to the electrical inertia of the inductor. When the pulse disappears, current starts flowing through both diodes from the power supply. Since both tunnel diodes have almost equal peak currents, and the diode in the low state already has additional current flowing through it, this tunnel diode will switch high, thereby changing the state of the flip-flop.

Coupling between stages is accomplished using a transistor. Whenever the output of the flip-flop goes to the high-voltage state (450 millivolts), it turns on the transistor and saturates it. The coupling transistor draws a small amount of current at all times and is operating in a class A mode. The emitter resistor is bypassed with a capacitor so that the transistor puts out a negative going pulse

which lasts until the capacitor charges up to the output voltage of the tunnel diode at which time the transistor turns off. This pulse momentarily switches both tunnel diodes in the second stage to the low state and a similar action, previously described, occurs. The L/R time constant in the flip-flop must be made large enough so the current is maintained longer than the pulse width of the coupling signals. Therefore, the value of the RC time constant is governed by the L/R time constant.

G. PULSE HEIGHT DISTRIBUTION MEASUREMENTS

The evaluation of the operation of the detector and counter described in Section II.F for random input signals was initiated by tests to measure the dark current output pulses of a 7746 photomultiplier mounted in a light-tight enclosure, as shown in Figure 5. A block diagram of the test setup is shown in Figure 10. Initially, some difficulty was experienced in coupling the detector circuitry to the counter. To ease this problem, the detector stage was slowed down to a 20 Mc rate by increasing the size of the inductor in the monostable circuit.

The first data to be taken with this setup was that required to verify the pulse amplitude distribution of dark current emission from the tube. The number of counts versus bias on the tunnel-diode threshold was recorded. In addition, data was also recorded for the output of the tube with the photocathode back biased. This test represents the dark current emission from all other structures in the tube and consists of a small number of pulses that increase approximately exponentially with decreasing amplitude. Data was also recorded for the pulse height distribution with a low level of illumination on the photocathode, as described in Section II.E.

The results of the three experiments are shown in Figure 11. The integral count versus threshold bias was plotted on a logarithmic scale, indicating two distinctly different regions of exponentially increasing counts with respect to bias.

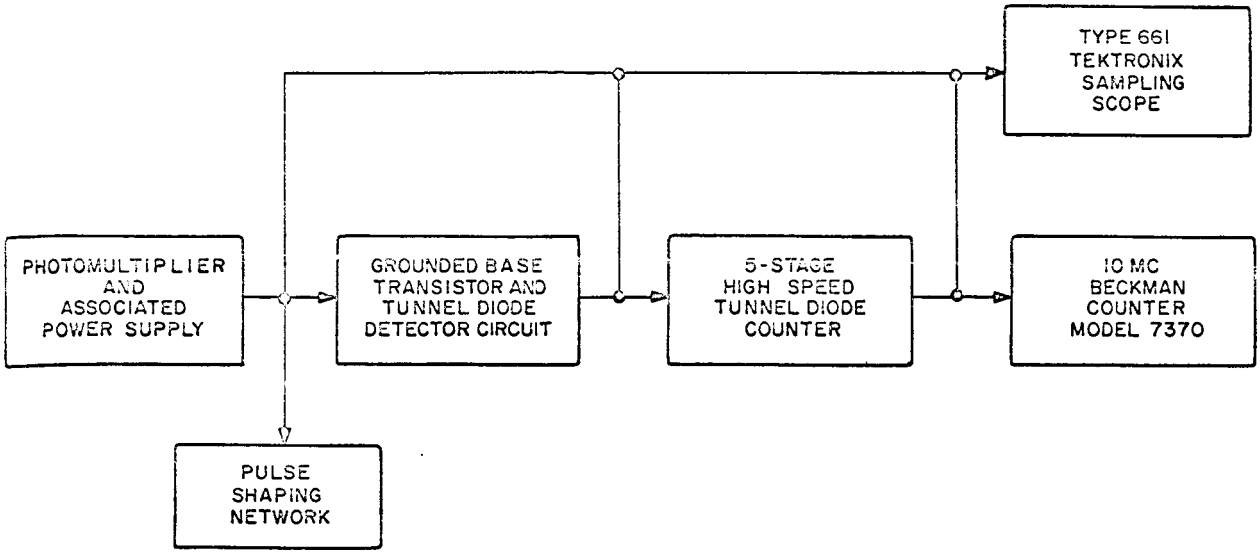

Figure 10. Diagram of Laboratory Test System

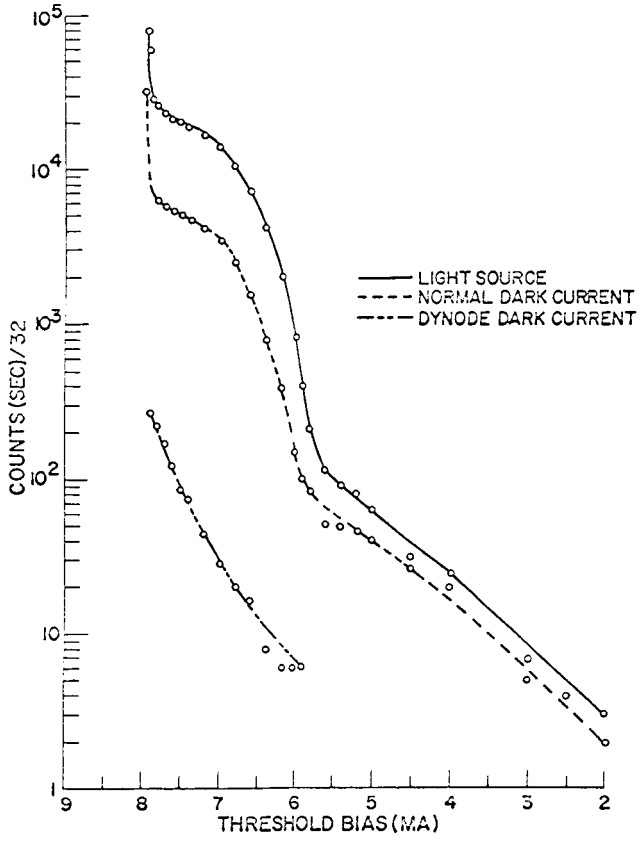

Figure 11. Pulse Height Distribution of 7746 Photomultiplier at 20 Mc

At the lower threshold biases of from 2 to 5.5 milliamperes, emission was exponential but with a different slope than at the higher threshold biases. This two-slope characteristic is thought to result from single and multiple emission from the photocathode.[3] The flattening out of the distribution curve for a threshold bias above 8 milliamperes is expected since a relatively small number of pulses occurs with amplitudes below that which represents minimum single electron emission from the photocathode. At very high biases (low threshold level), a sharp increase in number of pulses is observed corresponding to stray emission from dynodes and other structures within the tube.[4,5] If the integral curves are differentiated, a peak should occur which would indicate the pulse height of the most probable single electron pulse. The differential dark current pulse height distribution is shown in Figure 12, indicating a most probable pulse detected with a bias of 6.8 milliamperes.

H. COMPARISON OF DARK CURRENT MEASUREMENTS

It is possible to verify the most probable output value of a single election by comparing the results with measurements made of the dc anode current under similar conditions. A comparison was made to assure that the circuitry was actually detecting single electron emission from the tube. Assuming the reference threshold was 8.0 milliamperes and that the typical noise pulse was triangular in shape with a 6-nanosecond width, as shown in Figure 12, the average anode current can be calculated from the formulas

$$I_p = \frac{2 \epsilon A}{T} \tag{5}$$

where

ϵ = charge on electron = 1.6×10^{-19} coulomb

A = tube gain = 17×10^{c} @2,000V

I_p = peak anode current for single electron emission

T = typical pulse width = 6 nsec

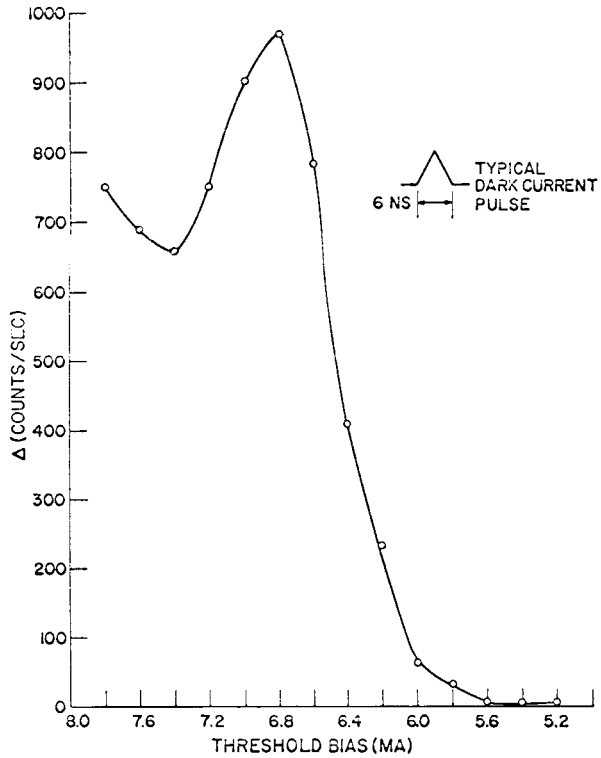

Figure 12. Differential Dark Current Pulse Height Distribution of 7746 Photomultiplier

and

$$I_{AV} = I_p \frac{T}{2} N \tag{6}$$

where

N = measured number of dark counts

= 224,000/sec

$$I_{AV} = 0.6\ \mu a$$

The agreement between measured and calculated values of the average dark current pulse amplitude was very close as the oscilloscope measured value was 1.2 microamperes. The average dark current measured was 1.0 microampere.

The value of N, which is the measured number of dark current pulses, is taken from the curve of Figure 11. The agreement between calculated and measured average dark current is quite close considering the fact that there is some dc leakage through the envelope of the tube which is not considered in the calculated value. In addition, the pulse height distribution curves of Figure 11 indicate some multiple electron emission from the photocathode also not included in the calculations. Inclusion of these factors would tend to make the results agree more closely.

I. PULSE HEIGHT DISTRIBUTION AT 250 MC

The speed of the detector circuit was increased to 250 megacycles by removing the large inductance. Pulse height distributions were recorded as in the previous case when the speed was 20 Mc. Since the average rate of dark current pulses and the average rate of single electron pulses from a weak light source should be small, no appreciable difference in counts versus threshold bias should result. However, as the data from the two runs were compared (see Figure 13), there was considerable disagreement. For example, at biases down 2 milliamperes or more from the threshold of the tunnel diode, the counts were lower and, as the bias approached the threshold, there was no flattening off of the curve but just a continuing increase in counts. The reason for these differences can be explained by two factors. First, a loss in sensitivity due to the smaller inductance now associated with the tunnel diode threshold circuit. Some signal is lost due to the lower impedance presented by this smaller inductance. This explains the lower counting rate at the lower biases but does not account for the swift increase in counts as the threshold is approached.

The second factor is ringing in the pulse. It can be seen, by looking at a photograph of a pulse output from the photomultiplier used in the tests (Figure 14) that the decaying portion of the pulse exhibits a certain amount of ringing. The ringing occurs at approximately 200 Mc. This ringing is associated with resonances caused in the anode structure and cannot be eliminated using the 7746

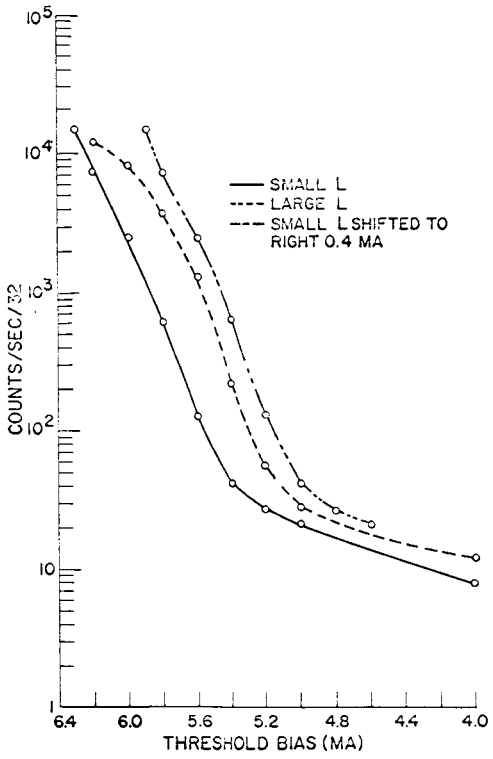

Figure 13. Pulse Height Distribution of 7746 Photomultiplier at 250 Mc

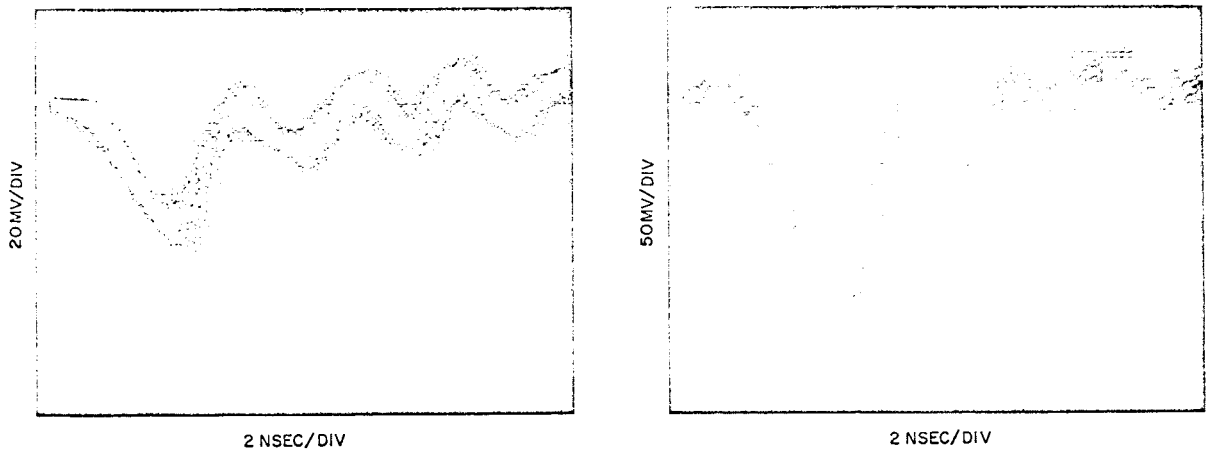

Figure 14. Dark Current Pulse from a 7746 Photomultiplier

photomultiplier tube. When the tunnel diode was operated at low frequencies (20 Mc), it was not bothered by the ringing as the tunnel diode did not recover in time, but, operating at higher speeds and at the higher threshold biases these ringing effects were detected and counted by the circuitry, thereby increasing the counting rates. The pulse extraction circuitry was not used in these tests. Also shown in Figure 13 is a reproduction of the pulse amplitude distribution curve shifted to the right by 0.4 milliampere to compensate for loss in threshold sensitivity at the higher counting rate. This curve closely follows the lower frequency pulse height distribution except as noted at the highest threshold biases. Ringing in the anode structure can be eliminated by proper design as has been attempted in the C-31000 tube.

J. RANDOM COUNTING TESTS

To verify the capability of the detector and counter circuits to operate at high average rates, a series of tests was performed using the test setup shown in Figure 10. The tests consisted of limiting the counting capability of the counter by purposely slowing it down. Various photocathode illumination levels were then established on the basis of the last dynode current and total counts recorded. This process was repeated for counter speeds of 10, 50, 100, 150, 200 and 250 Mc at various threshold bias levels. A plot of the results for a threshold bias 2 milliamperes below the threshold is shown in Figure 15a. For the two lower curves, it can be seen that essentially no change in counts occurs when the maximum speed of the counter is increased from 10 to 250 Mc. From this observation, it can be concluded that the average detected pulse rate is considerably below 1 Mc for these rates. At the higher average rates, a considerable variation in counting rate is observed, indicating average rates in excess of 2 Mc. The last dynode current was monitored in these tests and is included with the curves. At higher biases, somewhat erratic readings were observed at the higher counting rates (Figure 15b).

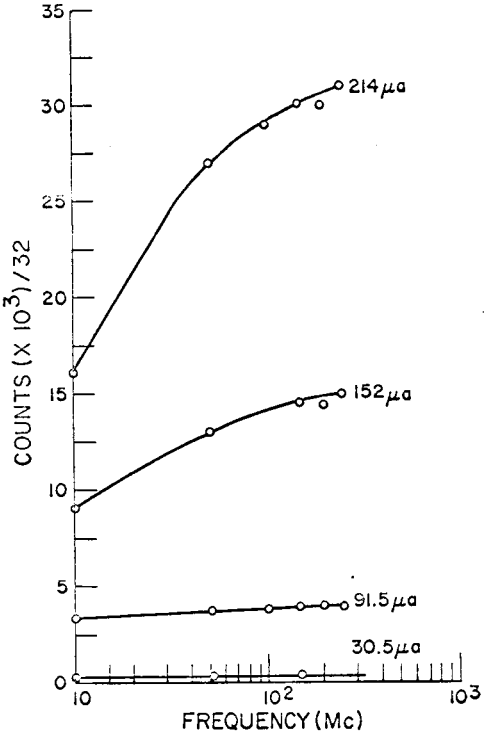

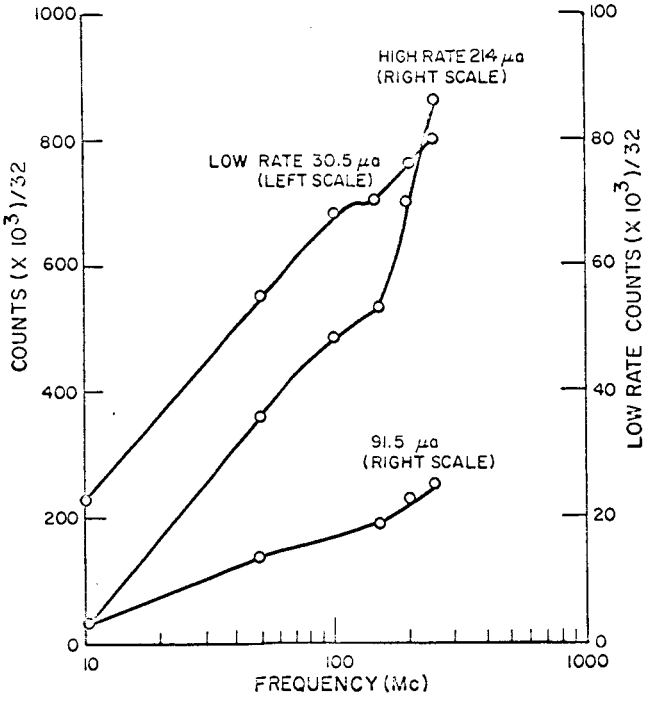

Figure 15. Random Counting Speeds

If the average rate of pulses is increased upward toward, say, 50 Mc, each curve should show a linear rising portion and then a flattening off at the higher frequencies. However, in these tests, instead of the curves flattening out, there seemed to be a tendency for the counts to increase at the higher rates and higher speed. These curves were taken without the pulse-shaping network and at a bias 0.5 milliampere down from the threshold. The reason for the high counts is probably due to a result of pulse pile-up and ringing at the anode.

Figure 14 shows the degree of ringing encountered with the photomultiplier used in these tests (7746). Figure 16 shows typical dark current pulses from the ruggedized type C7151H planned for actual use in the equipment. It can be seen that the ringing is much more pronounced in the 7746. The photographs of the C7151H pulses were taken at the laboratory test set-up at the Goddard Space Flight Center. When the pulse-shaping network was used in conjunction with this tube, very little ringing was produced.

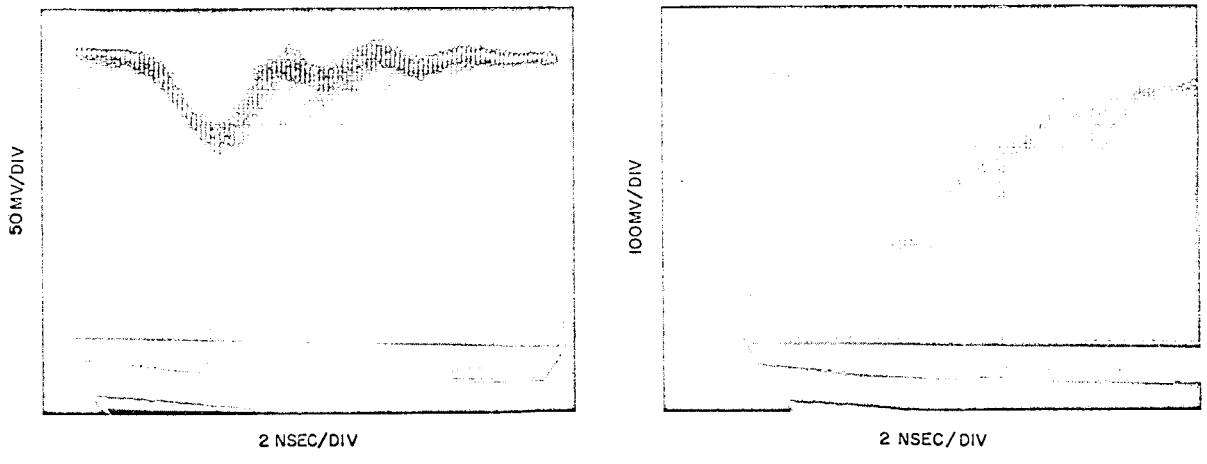

Figure 16. Typical Dark Current Pulses from a C7151H Photomultiplier

K. ADDITIONAL RANDOM TESTS

The breadboard detector and counter were tested in conjunction with NASA personnel at Goddard. A Nickel 63 beta source was mounted on a movable platform to produce emission for a plastic scintillator/photomultiplier combination mounted in a vacuum. The particle count was measured as a function of threshold bias with the source distance as a parameter. Some of the objects of the experiment were: (1) to find the relationship between the count (N) vs. voltage (V) with distance (d) as a parameter; (2) to verify that for a fixed V, the count N is related to d by the inverse square law. Let it be assumed that N follows the relationship

$$N = \frac{K_1}{d^2} A^{K_2 V} \tag{7}$$

where A, K_1 and K_2 are constants.

After taking the log on both sides,

$$\log N = \log \frac{K_1}{d^2} + V (K_2 \log A) \tag{8}$$

Let $\log N = y$, $\log (K_1/d^2) = b$ = constant, $K_2 \log A = m$ and $V = x$ then Equation 8 reduces to

$$y = b + mx \tag{9}$$

which is the equation of a straight line where m is the slope. The validity of Eq. 7 is verified by the fact that the experimental results of Figure 17 shows a straight line relationship. Here, the slope m is a measure of detector sensitivity.

To show N versus d for constant V, Equation 7 may be written as

$$\log N = \log \left(K_1 A^{K_2 V} \right) - 2 \log d \tag{10}$$

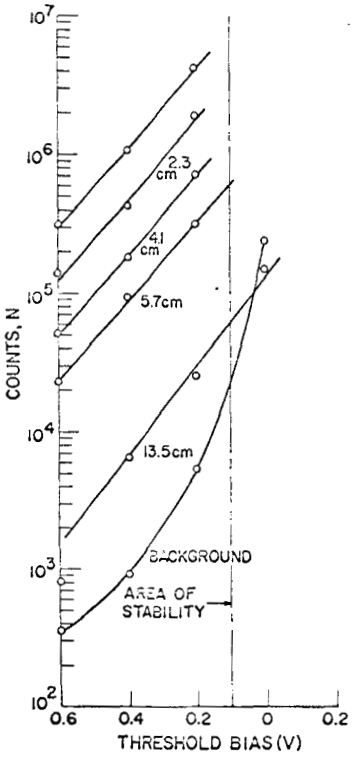

Figure 17. Particle Count as a Function of Threshold Bias using a Ni 63 Source

Let $\log N = y$, $\log (K_1 A^{K_2 V}) = a = \text{constant}$, and $\log d = x$ then Equation 10 results in

$$y = a - 2X \tag{11}$$

which is also the equation of a straight line with a slope of -2. This relationship is verified by plotting log N versus log d as shown in Figure 18. Some deviation from the straight line relationship can be expected in Figure 18 because the source at small separations is not truly a point source. The observation of these deviations, however, is made difficult by experimental measurement inaccuracy.

A second set of tests was performed using a laboratory ion source. Average counting rates were read from the breadboard counter versus threshold bias.

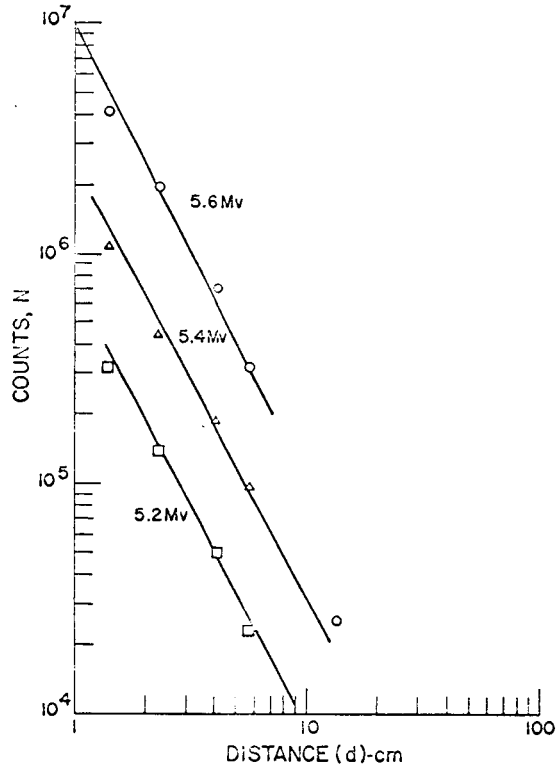

Figure 18. Particle Count as a Function of Distance

These results are shown in Figure 19 and Table I. Two average rates were calculated by measuring the ion stream separately. The calculated rates were 6.25 and 9 Mc. The respective counter readings were 7.7 Mc and 10.3 Mc. Attempts to increase this rate were unsuccessful due to relatively large resistors in the photomultiplier biasing network. A subsequent test was made with reduced biasing resistors, and good correlation between calculated values and counted pulses was achieved up to an average rate of 30 Mc.

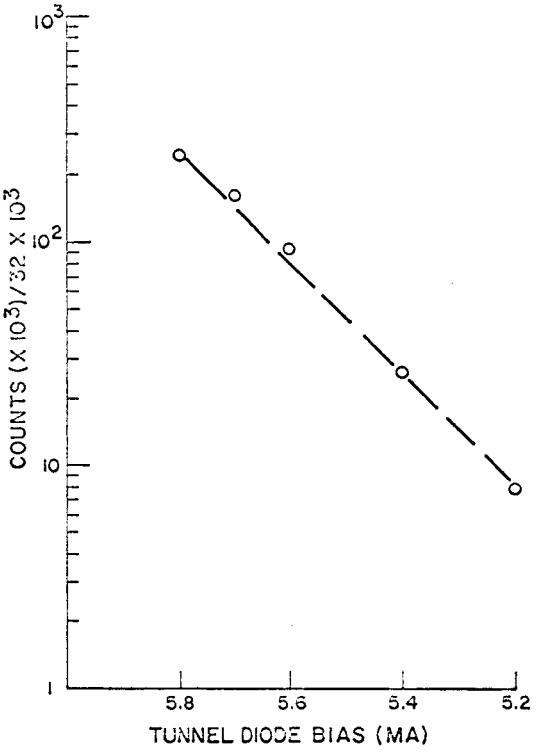

Figure 19. Particle Count as a Function of Threshold Bias Using an Ion Source

TABLE I. DATA RECORDED USING GODDARD ION SOURCE AND RCA DETECTOR-COUNTER CIRCUITRY

Bias (ma)	Average Counting Rates (Mc)	Background Counts	Ratio (x 10^3)
5.8	7.7	5120	1.56
5.7	5.12	3200	1.60
5.6	3.04	1340	2.26
5.4	0.865	608	1.42
5.2	0.256	192	1.33

SECTION III

CONCLUSIONS AND RECOMMENDATIONS

A. CONCLUSIONS

The ability to detect and count random events at average rates of the order of 50 Mc requires circuits with a high-speed random counting capability. Further, to obtain an accurate indication of the event statistics, a large percentage of the total events occurring should be detected and counted. For Poisson distributions with an average event rate of 50 Mc, pulse-pair resolution of 4 nanoseconds or 250-Mc counting rates or higher are required. A ratio of maximum counting rate to average counting rate of 5 to 1 results in over 80 percent counting efficiency; for a ratio of 10 to 1, the counting efficiency increases to 90 percent.

In this study, combinational tunnel-diode/transistor switching circuits have been investigated as the means of providing this high counting rate. A breadboard detector and five-stage counter were constructed and evaluated using both well-defined and random inputs. The results of the testing indicated an ability to detect and count pulses with separation less than 4 nanoseconds and to efficiently count random events at average rates in excess of 30 Mc. Using special pulse extraction techniques, a wide dynamic range of inputs in excess of 20 db were accommodated without loss of pulse-pair resolution capabilities.

A considerable effort was expended in obtaining test sources for the breadboard which realistically simulated the conditions to be encountered in actual usage. Two techniques for generating extremely narrow (a few nanoseconds) pulses of light were evaluated and utilized in determining the response of photomultipliers as well as the succeeding circuitry. A problem of ringing in the anode structure of some photomultipliers at a rate of approximately 200 Mc was encountered and found to cause

multiple counting of single events. This problem was found to be most severe, however, when counting single electron events such as photomultiplier dark current. Subsequent testing at NASA Goddard, with a source which included the effects of scintillator decay using a C7151H-type tube, showed that this was not a serious problem.

To evaluate the sensitivity of the breadboard, pulse height distribution measurements were made of the dark current of a representative photomultiplier with verification of the ability to detect single electron photocathode emission. Measurements of random single electron emission at higher rates were also obtained by the use of low-level stimulation of the photocathode. As a final test of the high-speed counting capability of the circuitry, random sources with average rates in excess of 30 Mc were used for evaluation. The results obtained were in close agreement with calibrations. Throughout the tests, no problems were encountered with the stability and reliability of the breadboard detector and counter.

B. RECOMMENDATIONS

Tests conducted both at RCA and NASA Goddard have demonstrated the feasibility of high-speed counting of pulses from photomultipliers at rates in excess of 250 Mc. The circuitry investigated has satisfied the basic requirements of speed, sensitivity and stability. In addition, optimized design is expected to result in a unit of atractively low-power dissipation, small size and low weight. Based on these conclusions, a program is recommended for the design of prototype units for environmental evaluation, followed by the construction of flight test units.

REFERENCES

1. Ogilvie, K.W; McIlwraith, N.; Zwally H.J.; and Wilkerson, T.D. "A Detector-Analyzer for Studying the Interplanetary Plasma" NASA Technical Note, NASA TND-2111, February 1964

2. "A Generator of Fast-rising Light Pulses for Phototube Testing" Lawrence Radiation Laboratory, University of California, Berkeley

3. Baicker, J.A. "Dark Current Photomultiplier" IRE Trans on Nuclear Science, NS-7 (1960)

4. Eberhardt, E.H. "Multiplier Phototubes for Single Electron Counting" IEEE Trans on Nuclear Science, June 1964

5. Bay, Z., Papp, G. "Determination of the Probability Distribution of the Number of Secondary Electrons," IEEE Trans on Nuclear Science, June 1964

Errata Sheet

FINAL PROJECT REPORT

FOR

HIGH-SPEED COUNTING OF PHOTOMULTIPLIER PULSES
(31 July 1964 - 30 September 1964)

1. Page 14, line 19 should read:

   The counter stages are chow-type flip-flops in the locked-pair configuration.[6]

2. Page 20, bottom line should read:

   1.2 milliamperes instead of 1.2 microamperes.

3. Page 32, add reference:

   6. Bush, Edgar G., " A Tunnel-diode Counter for Sattelite Applications", NASA Technical Note D-1337.